HHS Public Access

Author manuscript

J Photochem Photobiol B. Author manuscript; available in PMC 2017 September 15.

Published in final edited form as:

J Photochem Photobiol B. 2008 December 11; 93(3): 162–171. doi:10.1016/j.jphotobiol.2008.07.011.

UVA-induced photo recovery during early zebrafish embryogenesis

Qiaoxiang Dong[a,b,d], **W. Todd Monroe**[a], **Terrence R. Tiersch**[b], and **Kurt R. Svoboda**[c,*]

[a]Department of Biological and Agricultural Engineering, Louisiana State University and LSU Agricultural Center, Baton Rouge, LA 70803, USA

[b]Aquaculture Research Station, Louisiana State University Agricultural Center, Louisiana Agricultural Experiment Station, Baton Rouge, LA 70803, USA

[c]Department of Biological Sciences, Louisiana State University, Baton Rouge, LA 70803, USA

[d]School of Environmental Science and Public Health, Wenzhou Medical College, Wenzhou 325035, PR China

Abstract

DNA photorepair has been widely studied in simple aquatic organisms that live in the marine environment, but is less understood in more complex species that live in freshwater. In the present study, we evaluated UVA-induced DNA photo recovery in embryonic stages of zebrafish, *Danio rerio*, a freshwater model species. Evaluation of UVB exposure and UVA photo recovery of zebrafish embryos revealed different UVB tolerances and capacities for UVA photo recovery at different stages of development. Effective UVA photo recovery was observed at 3 h post-fertilization (hpf), 6–7 hpf, and 12 hpf, but not in the early cleavage stage (2–32 cells). UVA photo recovery was most effective during the gastrula stage (6–7 hpf) of development, and less effective at earlier stages (e.g., 3 hpf) or later stages (e.g., 12 hpf). Embryos at the cleavage stage of development were found to be tolerant to extreme levels of UVB exposure, and possible mechanisms were discussed. For embryos at 6–7 hpf, examination of time window (or delay of UVA exposure) that would still permit recovery from UVB exposure suggested a short time period of 2 h. The transgenic *fli-1* zebrafish with fluorescent vascular structure was used to show that embryos with normal morphological appearance could exhibit a disrupted vascular patterning, suggesting that this endpoint could provide a sensitive tool for detection of UV damage.

Keywords

Danio rerio; Ultraviolet radiation; UVA; Photo recovery Gastrulation; Fli-1

1. Introduction

Photo-reactivation was discovered at the organismal level serendipitously in 1949 during the study of UV-induced mutagenesis. Unexpected results were obtained that were attributed to

*Corresponding author. Tel.: +1 225 578 7469; fax: +1 225 578 2597. ksvobo1@lsu.edu (K.R. Svoboda).

an enhanced survival of UV-irradiated *Streptomyces griseus* conidia after illumination with visible light [1]. Since then, the biochemical mechanisms responsible for photoreactivation, known as DNA photorepair, have been elucidated [2,3] and documented in a variety of organisms, ranging from bacteria to multicellular eukaryotes [4]. While shorter wavelengths of UV (<320 nm) are responsible for the majority of DNA damage, UVA (400–315 nm) and visible light are known to drive the process of photorepair (see [5] for review). The fidelity and rate of photorepair differs widely among eukaryotic species, and also with age of the developing organism [6,7]. The general trend observed is that adults are more tolerant to UV than juveniles and developing zygotes, and that photoreactivation capability decreases with age [8,9].

Although there are previous studies of photoreactivation in aquatic organisms, DNA photorepair is less well studied in freshwater animals [10]. Zebrafish (*Danio rerio*) are freshwater fish whose small size, fecundity, embryonic transparency, and rapid development have led to their selection as a popular model vertebrate. Numerous mutant strains and transgenic lines of zebrafish have been created which have proved useful in studying aspects of development biology in basic and biomedical science [11–15]. These attributes also make it an excellent model for studies of DNA repair [16].

Previously, we have demonstrated the existence of a competent photorepair system in zebrafish embryos [17]. UVA wavelengths can effectively stimulate photoreactivation, yet the specific action spectra for proteins implicated in mediating photorepair in zebrafish are unknown. The closest known long wave absorbers in zebrafish are cryptochromes, which show only weak regulation of photolyase activity [18] and coincident with patterns of circadian rhythms [19]. The present study continued our investigation of UV exposure and photo recovery in zebrafish embryos. Specifically, we investigated the UVA photo recovery capability and efficiency across different developmental stages, and the time window of UVA photo recovery for UVB-irradiated gastrulated embryos, which was evaluated for the first time in a DNA photorepair study. Transgenic zebrafish expressing GFP in the vasculature system were also evaluated and determined to be a sensitive indicator of abnormalities caused by UVB irradiation at lower doses, as well as a sensitive diagnostic tool to evaluate UVA photo recovery. Correlations between UVB tolerance and the onset of photo recovery were also made in developing zebrafish embryos.

2. Materials and methods

2.1. Fish husbandry and embryo collection

Wild-type zebrafish were purchased from EkkWill Waterlife Resources, Gibsonton, FL (hereafter referred to as “pond-raised”), while transgenic *Tg(fli-1:EGFP)* (“*fli-1*”) fish were obtained from Dr. Brant Weinstein of the National Institute of Child Health and Human Development. *Fli-1* is an endothelial marker and GFP has been conjugated to the *fli-1* promoter. The GFP permitted observation and analysis of vasculature structure formation during zebrafish embryogenesis. Healthy fish were raised and kept at standard laboratory conditions of 28 °C on a 14:10 dark/light photoperiod [20] in a recirculating system. The fish were fed three times daily with either the zebrafish diet (Zeigler) or live artemia (Aquatic Habitats, Apopka, FL). Embryos were collected from group spawns or paired

spawns, and were rinsed several times in embryo medium [20] containing penicillin–streptomycin (0.05%). Embryos at various developmental stages were used for experiments with an emphasis on embryos in the mid-gastrulation stage of development (6–7 h post-fertilization, hpf).

2.2. Ultraviolet radiation exposure

Ultraviolet radiation B (UVB) was supplied with a high performance transilluminator (TFM-20, UVP Inc., Upland, CA), which provided an irradiance of 5.19 mW/cm^2 at 302 nm (818-ST-UV detector, Newport Corporation, Irvine, CA). The broad output in the UVB region matches the absorbance spectra of the many targets affecting cellular processes, DNA, cell membranes, proteins [21] and in particular, the cyclobutane pyrimidine dimers (CPDs) that are corrected in photorepair [3]. Ultraviolet radiation A (UVA) was supplied with a high intensity (GreenSpot 100-W) super pressure mercury lamp with a 5 × 1000 mm light guide (American Ultraviolet, Lebanon, IN), which provided an irradiance at 4.2 cm of 0.705 W/cm^2 at 365 nm with a short bandpass and infrared filters. The short bandpass filter (SWP-2502U-400; Lambda Research Optics, CA) had a cutoff at 400 nm and transmittance greater than 90% at 365 nm. A heat-absorbing filter was also used to absorb potential infrared emittance (Schott KG-2; Germany), having a transmittance of greater than 85% at 365 nm and less than 10% at 1100 nm. A spectral characterization of the UVA light source indicated that ~60% fell within the range of 365 ± 8 nm [22]. Embryos were exposed to UVA in the bottom of a 35-mm diameter cell culture dish containing 3 ml of embryo medium. UVB exposures were administrated from bottom to up while UVA exposures were administered from top to down at a distance of 4.2 cm from the fiber to the bottom of the dish.

2.3. Criteria for evaluating photo-damage

Hatch, mortality, and malformation were used as evaluation criteria for the assessment of UV effects. Percent hatch was calculated as the number of embryos hatched within 5 days after fertilization divided by the total number of embryos. Percent mortality was calculated as the cumulative mortality of embryos within 5 days. Cessation of heartbeat and circulation were used as end points for mortality. Classification of malformations was described previously [17]. Briefly, larvae designated as being malformed typically had mildly twisted or kinked trunk deformities and slightly enlarged pericardial sacs. Severe malformation was characterized by significant trunk deformities and grossly enlarged pericardial sacs. Percent total malformation (or severe malformation) was calculated as the number of embryos having any deformities (or severe deformities) after hatch divided by the total number of embryos surviving at 120 hpf. For treatment groups with 100% mortality before hatch, percent total and severe malformation were considered to be 100%. Embryos were examined daily for developmental progress, hatch, mortality, and malformation. Dead embryos were removed, and embryo media was replaced.

2.4. Assessment of UVA photo recovery on embryos at various stages of development

Embryos were exposed to various doses of UVB and subsequent UVA irradiation at the following developmental stages: 2–32 cell, 3 hpf, 6–7 hpf, and 12 hpf. For each exposure, a minimum of two replicates was performed with each replicate containing 20 embryos. After

the exposures, the embryos were incubated in a regular photoperiod as described in Section 2.1.

2.5. UVA photo recovery time window for embryos during mid-gastrulation

To determine the time window (or delay of UVA exposure) that would allow for recovery from UVB exposure, embryos were exposed to UVB and then UVA (either 211.5 or 338.4 J/cm^2) immediately (0 h) or after a delay period following the UVB exposure. For the lower UVB exposure dose (0.93 J/cm^2), the delay intervals at which UVA was delivered were 0.5, 1, 2, 4, and 6 h after the UVB exposure. For the higher UVB exposure dose (1.56 J/cm^2), the delay periods at which UVA was delivered were 0.5, 1, 2, 3, and 4 h after the UVB exposure. During the waiting periods, embryos were incubated in the dark. Controls included embryos exposed to UVB but without subsequent UVA irradiation, and embryos that did not receive UV irradiation. For controls not exposed to UV irradiation, 20 embryos were incubated in the dark for the first 20 h (referred to as “dark control”), and another 20 embryos were incubated in the light (referred to as “light control”) with regular photoperiod. All experiments were replicated a minimum of two times each with 20 embryos per treatment.

2.6. UV exposure for embryos collected from transgenic zebrafish

Fli-1 embryos at the mid-gastrula stage were exposed to UVB radiation for 1, 3, 5, and 10 min at a dosage of 0.31 J/cm^2 per min. This experiment was replicated three times (N = 60). Photo recovery studies were also performed where *fli-1* embryos were exposed to various doses of UVB and subsequent UVA irradiation at the 2–32 cell, 3 hpf, 6–7 hpf, and 12 hpf stages of development. After the exposures, embryos were incubated with a regular photoperiod as described under Section 2.1.

2.7. Microscopic examination of vascular patterning in transgenic fish after UV exposure

To determine if UV irradiation affected vascular patterning of *fli-1* fish, embryos at 6–7 hpf were exposed to UVB for 1 and 3 min at a dosage of 0.31 J/cm^2 per min. For the 3 min UVB exposure, half of the embryos were also exposed to UVA for 3 min at a dosage of 42.3 J/cm^2. In control experiments, embryos were exposed to UVA alone for 8 min. After exposure, embryos were incubated in a regular photoperiod with daily embryo medium changes and raised to larval stages of development. They were fixed with 4% paraformaldehyde in 0.1 M phosphate buffer (see [20] for recipe) and processed for microscopic analysis. The same procedure was also performed for 2–32 cell *fli-1* embryos with the only change being the intensity of the UVB and UVA doses used.

Images of GFP positive, *fli-1* larvae (72–120 hpf) were acquired digitally with a an ORCA-ER camera (Hamamatsu Photonics) mounted to an inverted microscope (Zeiss Axiovert 200M) with epi-fluorescence capabilities. The GFP filter cube on the microscope was used to acquire the GFP fluorescence signal. These digital images were acquired in the trunk region over the yolk sac extension. Typically, 5–7 segments in each field of view were imaged utilizing a 20×, dry-objective with a 0.4 numerical aperture. In some cases, optical sections (z-stacks) were obtained through the region of interest with a 40× oil objective (1.3 numerical aperture). Each section was acquired with a Zeiss ApoTome placed in the light

path of the microscope. These stacks were reconstructed and projected in three-dimensional volumes using Imaris 5.72 (Bitplane, Inc.).

2.8. Data analysis

For dose responses, the concentration causing 50% mortality (LD_{50}) was calculated with logistic regression (Logit model). For other experiments, data were analyzed using one-way analysis of variance (ANOVA) (SAS 9.0, SAS Institute Inc., Cary, NC). When a significant difference ($\alpha = 0.05$) was observed among treatments, Tukey's Honestly Significant Difference Procedure was used for pair-wise comparisons. Results were presented as means ± SD, and probability values of $P < 0.05$ were considered to be significant. Percentage data for hatch, mortality, malformation, and severe malformation were arcsine-square root transformed prior to analysis.

Because of the variability of embryo quality at the 2–32 cell stage of development, data obtained at this stage were normalized to the controls. For percent mortality and hatch, data were normalized by subtraction of control values. For percent hatch, data were normalized by division with the control values. Negative values were considered to be 0, while percentages higher than 100% were considered as 100%. Percentage of recovery was calculated based on the formula: $R = (t_1 - t_2)/t_1 \times 100$ for mortality and malformation, and $R = (t_2 - t_1)/(1 - t_1) \times 100$ for hatch where R represents percentage of recovery, and t_1 are means of UVB treatment only, and t_2 are means for treatment after UVA photo recovery; R was considered to be 0 when negative values occurred. A higher R value represents better efficiency of photo recovery.

For the transgenic *fli-1* fish, the additional end point of inter-segmental blood vessel (ISBV) morphology was analyzed. Images of larvae containing GFP positive ISBVs were magnified until the myotome segments were easily visible. By 48 hpf, the patterning of ISBVs within the zebrafish vasculature system is highly organized where each hemi-segment along the anterior–posterior axis contains one ISBV [23]. ISBVs have a very characteristic "S" profile when the embryo is mounted laterally. In control and UV-exposed larvae, the number of ISBVs in a region of interest, over yolk sac extension that exhibited this "S" profile was divided by the total number of segments analyzed in that region of interest. In control zebrafish older than 48 hpf, this would yield 100% percent normal ISBVs. For ISBV morphology data obtained from UVB-exposed embryos, the typical phenotype observed was that individual ISBVs did not exhibit the characteristic "S" profile. Instead they projected in a straight line along the dorsal–ventral axis. Thus, the percent normal ISBVs in the UVB-exposed larvae when quantified is less than 100% if the exposure produces an abnormal phenotype. This type of analysis has been used previously by others studying nervous system patterning in embryonic zebrafish [24,25]. All ISBV data were analyzed using either Kruskal-Wallis one-way analysis of variance (ANOVA), or when appropriate, the Student's *T*-test. Values are presented as means ± standard error. Probability values of $P < 0.05$ were considered to be significant.

3. Results

3.1. Assessment of UVA-induced photo recovery in embryos at different stages of development

The degree of UVA photo recovery following UVB exposure varied with developmental stage and UVB dose (see Supplemental Table 1). During the rapid cell division stage (2–32 cell stage), embryos could tolerate UVB irradiation as high as 6.22 J/cm^2 while still maintaining a ~65% hatch rate (Table 1). However, using the endpoint criteria of mortality, percent malformation and hatch rate, the ability to photo recovery was not evident at this early stage ($P > 0.05$). Embryos at later stages of development had a decreased tolerance to UVB irradiation. The most vulnerable stage of UVB tolerance was observed in embryos at 12 hpf. The ability to photo recovery with UVA was observed as early as 3 hpf. However, it was less efficient than the photo recovery capacity observed at later developmental stages (Fig. 1). At 12 hpf, UVA photo recovery was less effective at the high doses of UVB irradiation compared to the low doses. For example, when 12 hpf embryos were exposed to 0.93 J/cm^2 of UVB, percent recovery from mortality was 52% and from severe malformation was 48%. If 12 hpf embryos were exposed to 3.11 J/cm^2 of UVB, percent recovery was virtually nonexistent for mortality (3%) and severe malformation (0%). However, if these high doses of UVB were coupled with UVA exposure during the mid-gastrula stage of development (6–7 hpf), embryonic capacity for photo recovery was evident, for example, percent recovery of mortality was 93% (Fig. 1).

3.2. UVA photo recovery time window for embryos exposed during the mid-gastrula stage

For embryos exposed to 0.93 J/cm^2 UVB, photo recovery was observed if the UVA was delivered within 2 h of the UVB exposure (Fig. 2). In embryos exposed to UVB alone, percent hatch was significantly lower ($P < 0.006$) than in control embryos or those embryos that were exposed to UVA within a 2-h time window following the UVB exposure (Fig. 2). When the delay between the UVB exposure and UVA was extended to 4 h or greater, photo recovery was not observed. This was true for the hatch rate and mortality endpoints. Exposure to 0.93 J/cm^2 UVB also resulted in malformations in 99 ± 2% of the embryos analyzed. However, when UVA was delivered immediately after the UVB exposure, the percentage of malformations observed in embryos decreased to 22% (Fig. 2). Similar to the observations of percent mortality and hatch, increasing the delay in the delivery of UVA exposure reduced the efficiency of photo recovery for the malformation endpoint.

Varying the dose of UVA also influenced the duration of the delay window that resulted in photo recovery of the malformation endpoint. When UVA (211.5 J/cm^2) was administered within 1 h after UVB exposure, a significant reduction of percent malformation was observed in the larvae ($P < 0.05$, Fig. 2). When a higher UVA dose (338.4 J/cm^2) was delivered within 2 h after the same UVB exposure, the capacity to photo recover was evident as a significant reduction in percent malformation (Fig. 2). However, when the higher UVA exposure was delivered 4 h or later after the UVB exposure, photo recovery was not evident, similar to that observed with the lower UVA dose.

At a higher dose of UVB (1.56 J/cm^2, see Supplement Fig. 1), a time window for UVA photo recovery was still evident. Percent hatch was significantly higher ($P < 0.001$) in larvae with UVA photo recovery than in those exposed to UVB irradiation alone (48 ± 10%). However, the maximal delay period for effective UVA photo recovery (i.e., showing significant difference) of severe malformation was further reduced to 0.5 h when lower UVA doses were used to induce photo recovery. If higher doses of UVA were used to induce photo recovery, the delay between the UVB exposure (1.56 J/cm^2) and the subsequent UVA exposure that resulted in successful photo recovery was 1 h. In terms of total malformation, a low dose of UVA (211.5 J/cm^2) did not induce photo recovery even when the exposure was done immediately after the UVB radiation. Successful photo recovery was observed at a higher UVA dose, but this UVA exposure had to occur immediately after the UVB exposure. Control embryos without UV radiation had 100% hatch, and 0% malformation.

3.3. UV exposure in transgenic zebrafish embryos

The characterization of UVA-induced photo recovery in the initial part of this study used three different UVB-induced endpoints and tested reversibility of those endpoints by UVA exposure. The endpoint of mortality was the easiest assessment, however, this criterion was not as straightforward when assessing photo recovery in young embryos at the cleavage stage (2–32 cells). Embryos at this early stage showed little mortality with UVB exposures, even when exposed to a dose of 4.67 J/cm^2 (Table 1). Because these embryos showed normal morphology even at high doses, we sought a more sensitive endpoint to evaluate photo-damage and photo recovery. We chose to analyze internal structures in transgenic zebrafish expressing GFP in the vascular system. Because the vasculature in zebrafish has a very patterned and organized stereotypical appearance, disruptions in this patterning caused by UVB exposure were easy to analyze.

Prior to the photo recovery studies, we established the UVB tolerances of *fli-1* transgenic embryos in the mid-gastrula stage as well as the 2–32 cell stage of development. Similar to pond-raised fish, decreases in hatch rate, and increases in mortality and occurrence of malformations in *fli-1* fish were observed when exposing 6–7 hpf embryos to increasing UVB doses (Fig. 3). Embryos exposed to a dose of 1.56 J/cm^2 or higher UVB radiation had significantly lower hatch rates and higher mortality and malformation rates when compared to embryos exposed to the lower doses of UVB ($P < 0.05$). Although there were no significant differences in percent hatch and mortality at doses of 0, 0.31, and 0.93 J/cm^2, 74 ± 28% of the embryos exhibited malformations when exposed to 0.93 J/cm^2 UVB. This is in contrast to stage-matched controls not exposed to UVB radiation where only 2 ± 3% ($P < 0.05$) were malformed. The calculated LD_{50} of UVB radiation for embryos of *fli-1* zebrafish exposed at the mid-gastrula stage was 1.41 J/cm^2.

Similar to the pond-raised fish, *fli-1* embryos exhibited the same ability to tolerate UVB irradiation across different development stages. In brief, embryos at the 2–32 cell stage exhibited the highest tolerance to UVB. For example, a UVB exposure dose of 1.56 J/cm^2 which produced 80% mortality when the exposure was delivered during the mid-gastrula stage did not induce mortality when delivered at the 2–32 cell stage (60/60 embryos survived). As in the case of the pond-raised fish, significant mortality and malformation

were not detected until a UVB dose of 4.67 J/cm^2 was used (Table 1). Moreover, *fli-1* embryos at the 2–32 cell stage exhibited a lack of UVA photo recovery capacity similar to the pond-raised fish. At this early developmental stage, UVA-induced photo recovery capacity, when assayed with the mortality, hatch rate, or percent malformation endpoints, was non-existent (Table 1). UVA photo recovery was first observed as early as 3 hpf (1000 cell stage) in *fli-1* embryos, but was less efficient than at later stages of development (data not shown).

3.4. Microscopic examination of vascular patterning of transgenic fish after UV exposure

The expression of GFP is robust in the *fli-1* transgenic zebrafish line and the vascular system where the GFP is expressed develops in a highly organized and patterned fashion [23] that can be detected in fixed tissues. The patterning of the vasculature is shown in Fig. 4 where a zebrafish larva has been optically sectioned and projected at different angles offering a perspective of the patterning. A characteristic “S” pattern of the ISBV along the dorsal–ventral axis occurs within each trunk segment along the larva (Fig. 4B).

In pond-raised zebrafish embryos, UVA exposure at mid-gastrulation (338.4 J/cm^2) had no adverse effect on embryonic development. UVA exposures as high as 846 J/cm^2, did not induce abnormalities in these fish (see Supplement Fig. 2). The UVA tolerances of *fli-1* embryos were also established. In *fli-1* embryos, an exposure of 126.9 J/cm^2 or 338.4 J/cm^2 UVA during the mid-gastrulation did not disrupt gross morphology or the vasculature by the larval stage of development (Fig. 5A, top and middle). However, the 338.4 J/cm^2 UVA dose caused a developmental delay in 14 of 60 embryos (data not shown). These embryos were more similar in appearance to 22–23 hpf embryos when observed at 29 hpf. Thus the 126.9 J/cm^2 UVA dose was the dose chosen for studies in mid-gastrula stage *fli-1* embryos.

A threshold of UVB exposure that resulted in vasculature disruption was also determined in *fli-1* embryos. UVB exposure (0.31 J/cm^2) during the mid-gastrulation resulted in ~5% mortality (Fig. 3). In the surviving larvae, ~15% of the ISBVs analyzed were abnormal (Fig. 5A, bottom, B). Although this was a significant difference, we chose to perform photo recovery experiments with a higher level of UVB exposure to better differentiate between photo-damaged and recovered vasculature. When the UVB dose was increased to 0.93 J/cm^2, the mortality increased, but only to ~20% (Fig. 3). However at this dose, the vasculature was severely disrupted in the exposed larvae. Many of the ISBVs analyzed failed to exhibit the characteristic “S” profile. Instead, they projected in a straight trajectory from the dorsal to ventral portion of the larva (Fig. 6). This phenotype was true for larvae that had either abnormal or normal gross morphologies when compared to stage-matched controls (data not shown). Photo recovery was achieved with subsequent UVA exposure (126.9 J/cm^2) as the ISBVs in larvae exposed to 0.93 J/cm^2 UVB followed by UVA were similar in appearance to those ISBVs in control larvae (Fig. 6A, bottom, B).

We also tested photo recovery capacities in the *fli-1* embryos exposed to UVB during the cleavage stage (2–32 cells) using the vasculature system as the endpoint. As indicated earlier, embryos from pond-raised or *fli-1* fish were able to tolerate high doses of UVB when assayed with mortality, percent hatch or malformation indices. But in *fli-1* embryos, a UVB exposure of 1.56–4.67 J/cm^2 produced detectable abnormalities in ISBVs when observed at

the larval stage of development (Fig. 7). At the high dose of 4.67 J/cm^2 UVB, 59 ± 11% of the vessels exhibited the characteristic “S” profile (Fig. 7B) compared to 99% of controls. This high dose also produced spacing irregularities between vessels that were not photo-recovered by UVA exposure (data not shown). At the lower doses of UVB (1.56 or 3.11 J/cm^2), 70% of vessels analyzed exhibited the characteristic “S” profile (Fig. 7B). Attempts to restore the damaged vasculature in these 2–32 cell stage *fli-1* embryos were not successful with UVA exposure occurring immediately after the UVB exposure (Fig. 7A, bottom, B). Finally, when UVA (338.4 J/cm^2) was delivered alone at the 2–32 cell stage, the overall vascular patterning in the larvae was not altered (Fig. 7A, top, B). However, in some instances, the ISBVs were thinner although they exhibited their characteristic “S” profile and in other cases, the vessels exhibited ectopic branches (data not shown). In all segments analyzed (n = 99), the spacing between ISBVs and the patterning of individual vessels were not severely altered by UVA exposure alone at the 2–32 cell stage.

4. Discussion

In the present study, we observed in zebrafish embryos different types of responses to UV exposure, either dependent or independent of UVA photo-reactivation. Without subsequent UVA exposure, embryos at the cleavage stage were found to be more tolerant to high levels of UVB than embryos during gastrulation and segmentation stages of development. This could be due to dark repair processes, maternal gene products passed onto the developing egg or the chorion itself acting as a protective barrier which absorbs UVB radiation. In the case of invertebrate eggs, UV-absorbing maternal gene products can be passed on to embryos allowing them to survive the early stages of development [26]. Studies have also indicated that the fish chorion and the developing embryo can contain low molecular weight compounds, such as gadusol, which absorb UV radiation [27,28]. Although we have not identified this maternal product, our results are consistent with an early protective mechanism in the zebrafish egg that is likely not the product of zygotic transcription, but may have been passed on from the female to the embryo.

As suggested, the chorion may play a role as a primary defense to UVB exposure up to the cleavage stage of development. Mechanical studies indicate that the stiffness of the zebrafish chorion decreases through development [29]. Studies with Nile tilapia *Oreochromis niloticus* showed that embryos dechorionated at early stages (e.g., cleavage or blastula) could not survive into adulthood [30]. This indicates that the chorion plays a more important role in protection to the cleavage stage than in later stages of development. In contrast to responses to UVB exposure, zebrafish embryos at earlier stages of development have been shown to be more sensitive to chemical or chilling exposures (e.g. [31,32]) than later stages. This differential response to stressors at early developmental stages suggests that different mechanisms underlie tolerances to UV exposure, chemical insult, and temperature shock. It is possible that chemical exposure of embryos early in the cleavage stage may damage the chorion, thus leading to high mortality; while damage to the chorion at later stages would have less effect on embryo survival when its role is less critical. Moreover, when subjected to UV irradiation, the more elastic cleavage stage chorion combined with the fluid-filled perivitelline space may provide embryos with protection from UVB [33]. Our findings are

also in agreement with studies of calanoid copepod and Atlantic cod *Gadus morhua*, in which larvae were found to be more sensitive to UVB than eggs [33].

When the embryos reached the gastrulation stage of development, UVB tolerance decreased. However, the ability to recover from UVB-induced damage was most efficient at the mid-gastrula stage. Our previous study demonstrated that zebrafish embryos exposed to UVB irradiation during the mid-gastrula stage could be recovered with subsequent UVA exposure [17]. In the present study, zebrafish embryos at different stages of development exhibited different capacities for UVA photo recovery. Effective UVA photo recovery was observed at 3 hpf, 6–7 hpf, and 12 hpf, but not in the early cleavage stage of development (2–32 cells). UVA photorepair was most effective during the gastrula stage (6–7 hpf) of development, and less effective at earlier stages (e.g., 3 hpf) and later stages (e.g., 12 hpf). In the wild, zebrafish eggs are laid and fertilized just after dawn [34] thus embryos at 6–7 hpf (mid-gastrula stage of development) are generally exposed to the maximal solar UV. Under these conditions, the risk of DNA damage is likely to be high. Therefore, effective UVA photorepair would be necessary to increase survival at this time. High efficiency of DNA photorepair at the gastrula stage has been demonstrated recently in echinoid embryos, in which the highest repair rate of CPDs was found in the gastrula stage rather than in earlier (blastula) or later (pluteus) developmental stages [35].

Studies of gene expression in *D. melanogaster* found a high concentration of photolyase protein in embryos and adult ovaries, yet the photolyase gene was highly expressed only in ovaries [36]. This suggests that photolyase molecules transferred from ovary to eggs were able to protect eggs from harmful UV present in sunlight. Given what is known about zebrafish, a scenario comes to mind where this same mechanism may be present in embryos at the cleavage stage of development thus contributing to the survivability to UVB exposure. However, our observation that photo recovery cannot be induced by UVA exposure at the 2–32 cell stage may suggest otherwise. In addition, previous studies suggested that sensitivity to light in the early stages of zebrafish development not only leads to an increase in transcript levels of circadian genes, but also of genes involved in DNA repair [37]. Thus, embryos at the earliest stages of development appear to survive UV exposure better than those at the later segmental (12 hpf) stage of development.

In addition to developmental stage variations in photo recovery capacity, we evaluated dose thresholds for UVA-induced photo recovery in UVB-irradiated embryos. When embryos were exposed to UVB doses that were higher than the minimal lethal dose (e.g., 3.11 J/cm^2 for 12 hpf embryos), UVA photo recovery was minimal or non-significant. This suggested that when UVB-induced DNA damage exceeds a threshold, photo recovery is impossible or inefficient. However, when occurring within this threshold, effects of UVA photo recovery were most evident in rescuing heavily damaged embryos, and less noticeable at ameliorating less severe malformations. This trend is substantiated by a greater percent recovery for mortality and severe malformation than for mild malformations.

The present study also evaluated the time window for UVA-induced photo recovery for zebrafish embryos exposed to UVB at the gastrula stage of development. Our findings indicate that the ability to photo recovery is linked to the timing and dose of UVA exposure

following UVB exposure. Maximal photo recovery occurred in embryos exposed immediately to UVA irradiation following UVB exposure. A delay of 0.5–2 h produced recovery that was significantly higher than controls without UVA irradiation, which we referred to as the effective time window of photo recovery. However, a delay of more than 2 h in receiving UVA exposure for UVB-irradiated embryos did not result in significant recovery. Moreover, a smaller effective time window was observed with a higher UVB dose or a lower UVA dose. Our findings indicated that the DNA damage caused by UVB irradiation became irreversible if it was not repaired within a 2 h time frame. This also suggested that given these experimental conditions with UVA stimulation, photoenzymatic repair, rather than nucleotide excision repair or similar dark repair process, was the primary pathway responsible for recovery in UVB-irradiated zebrafish embryos.

Photo recovery and the ability to tolerate high levels of UVB appear to be inherently linked. It is apparent that as the embryo develops to the gastrula stage, it cannot tolerate UVB exposures as well as the cleavage stage embryo can. Coinciding with this decrease in UVB tolerance is an increased in photo recovery. As indicated previously, the enzyme photolyase can be detected at 3 hpf in zebrafish [37]. Although gastrulation begins at ~5 hpf in zebrafish raised at 28 °C, the cues to initiate gastrulation are present at about the 1000 cell stage (3 hpf) which coincides with the 10th cell division [38]. At this 3 hpf time point, mitosis rates decrease, cell movements are initiated, and most importantly, zygotic transcription begins. Thus, as photolyase expression is turned on, the UVB tolerances of the embryo may decrease. If UVA is present with UVB exposure as is the case in the wild, UVA would activate the photolyase and repair damage caused by UVB exposure. Therefore, it is possible that the ineffective or non-existent UVA-induced photo recovery at the cleavage stage may be due to the high resistance of UVB at that stage. The ability to photo recover coincides with the activation of zygotic transcription where the need to repair damaged DNA would be critical as cells begin to differentiate. Prior to differentiation, if a cell is damaged or dies, other cells may propagate to compensate for normal development [26,39]. Therefore, the ability of a developing embryo to exhibit regulative development may also contribute to its ability to have high UVB tolerances. Although this is somewhat speculative, this would ensure that the embryo would make it through the early phases of development where cells are undergoing multiple rounds of mitosis, but have not yet differentiated.

To test the absence of photo recovery capabilities in 2–32 cell stage developing eggs, we used transgenic zebrafish as a sensitive indicator of photo-damage. At this early time point, the mortality and malformation endpoints were not sensitive indices of UVB-induced damage because of the tolerance to high doses of UVB. The transgenic *fli-1* zebrafish, because of its fluorescent vascular system, provided an effective assay for evaluating UVB-induced damage. Similar to the pond-raised fish, effective UVA photo recovery in this transgenic fish was observed in embryos at 3 hpf and onward, but not in embryos at the cleavage stage (2–32 cells). More interestingly, the UVB-exposed zebrafish embryos at cleavage stage were found to have disrupted vascular patterning, although they appeared normal at the gross morphological level. This suggests that some signaling cascade associated with circulatory system patterning and development was affected by UV exposure, but this alteration did not seem to affect the overall development of the organism. This also demonstrated that the assessment of the vasculature system in *fli-1* embryos could

be used as a sensitive diagnostic indicator to evaluate UVB-induced damage and UVA-induced photo recovery. In future studies aimed at elucidating the molecular mechanisms of photo recovery, a more quantitative analysis will be necessary for accurate evaluation of damage associated with lower doses UVB radiation. However, for evaluating large numbers of embryos to assess UVB-induced damage, the *fli-1* line provides a useful screening tool.

Supplementary Material

Refer to Web version on PubMed Central for supplementary material.

Acknowledgments

This work was supported by the Louisiana State University Agricultural Center Biotechnology Education for Students and Teachers (BEST) Postdoctoral Fellowship to QD. We thank Dr. Brant Weinstein of the National Institute of Child Health and Human Development for providing the transgenic *fli*-EGFP fish, R. Tulley for administrative assistance, J. Forman, R. Blidner, M. Huguet, J. Casey, and M. Lapré for laboratory help and R. Pollet for fish care. This manuscript was approved for publication by the Director of the Louisiana Agricultural Experiment Station as number 2008-244-1850.

5. Abbreviations

UVA	ultraviolet A
UVB	ultraviolet B
CPDs	cyclobutane pyrimidine dimers
hpf	hours post-fertilization
ISBV	intersegmental blood vessel (includes intersegmental arteries and veins)

References

1. Kelner A. Effect of visible light on the recovery of *Streptomyces griseus* Conidia from Ultra-violet irradiation injury. Proc Natl Acad Sci USA. 1949; 35:73–79. [PubMed: 16588862]
2. Heelis PF, Kim ST, Okamura T, Sancar A. The photo repair of pyrimidine dimers by DNA photolyase and model systems. J Photochem Photobiol B. 1993; 17:219–228. [PubMed: 8492239]
3. Sancar A, Sancar GB. DNA-repair enzymes. Annu Rev Biochem. 1988; 57:29–67. [PubMed: 3052275]
4. Jeffrey, WH., Kase, JP., Wilhelm, SW. UV radiation effects on heterotrophic bacterioplankton and viruses in marine ecosystems. In: de Mora, S.Demers, S., Vernet, M., editors. The Effects of UV Radiation in the Marine Environment, Cambridge Environmental Chemistry Series. Vol. 10. Cambridge University Press; New York: 2000. p. 206-236.
5. Sinha RP, Häder DP. UV-induced DNA damage and repair: a review. Photochem Photobiol Sci. 2002; 1:225–236. [PubMed: 12661961]
6. Malloy KD, Holman MA, Mitchell D, Detrich HW. Solar UVB-induced DNA damage and photoenzymatic DNA repair in Antarctic zooplankton. Proc Natl Acad Sci USA. 1997; 94:1258–1263. [PubMed: 9037040]
7. Grad G, Burnett BJ, Williamson CE. UV damage and photoreactivation: timing and age are everything. Photochem Photobiol. 2003; 78:225–227. [PubMed: 14556307]
8. Lacuna DG, Uye S. Effect of UVB radiation on the survival, feeding, and egg production of the brackish-water copepod, *Sinocalanus tenellus*, with notes on photoreactivation. Hydrobiologia. 2000; 434:73–79.

9. Lacuna DG, Uye S. Influence of mid-ultraviolet (UVB) radiation on the physiology of the marine planktonic copepod *Acartia omorii* and the potential role of photoreactivation. J Plankton Res. 2001; 23:143–156.
10. Olson MH, Mitchell DL. Interspecific variation in UV defense mechanisms among temperate freshwater fishes. Photochem Photobiol. 2006; 82:606–610. [PubMed: 16613520]
11. Lieschke GJ, Currie PD. Animal models of human disease: zebrafish swim into view. Nat Rev Genet. 2007; 8:353–367. [PubMed: 17440532]
12. Fetcho JR. The utility of zebrafish for studies of the comparative biology of motor systems. J Exp Zool B. 2007; 308:550–562.
13. Zacchigna S, Tasciotti E, Kusmic C, Arsic N. In vivo imaging shows abnormal function of vascular endothelial growth factor-induced vasculature. Hum Gene Ther. 2007; 18:515–524. [PubMed: 17559317]
14. Beattie CE, Carrel TL, McWhorter ML. Fishing for a mechanism: using zebrafish to understand spinal muscular atrophy. J Child Neurol. 2007; 22:995–1003. [PubMed: 17761655]
15. Goessling W, North TE, Zon LI. New waves of discovery: modeling cancer in zebrafish. J Clin Oncol. 2007; 25:2473–2479. [PubMed: 17557959]
16. Sussman R. DNA repair capacity of zebrafish. Proc Natl Acad Sci USA. 2007; 104:13379–13383. [PubMed: 17686971]
17. Dong Q, Svoboda K, Tiersch TR, Monroe WT. Photobiological effects of UVA and UVB light in zebrafish embryos: evidence for a competent photorepair system. J Photochem Photobiol B. 2007; 88:137–146. [PubMed: 17716904]
18. Daiyasu H, Ishikawa T, Kuma K, Iwai S, Todo T, Toh H. Identification of cryptochrome DASH from vertebrates. Genes Cells. 2004; 9:479–495. [PubMed: 15147276]
19. Thompson CL, Sancar A. Photolyase/cryptochrome blue-light photoreceptors use photon energy to repair DNA and reset the circadian clock. Oncogene. 2002; 21:9043–9056. [PubMed: 12483519]
20. Westerfield, M. The Zebrafish Book. University of Oregon Press; Eugene, OR: 1995.
21. Buma, AGJ., Boelen, P., Jeffrey, WH. UV Effects in Aquatic Organisms and Ecosystems. In: Helbling, EW., Zagarese, H., editors. Comprehensive Series in Photochemistry and Photobiology. Royal Society of Chemistry; Cambridge: 2003. p. 291-329.
22. Forman J, Dietrich M, Monroe WT. Photobiological and thermal effects of photoactivating UVA light doses on cell cultures. Photochem Photobiol Sci. 2007; 6:649–658. [PubMed: 17549267]
23. Isogai S, Lawson ND, Torrealday S, Horiguchi M, Weinstein BM. Angiogenic network formation in the developing vertebrate trunk. Development. 2003; 130:5281–5290. [PubMed: 12954720]
24. Svoboda KR, Vijayaraghavan S, Tanguay RL. Nicotinic receptors mediate changes in spinal motoneuron development and axonal pathfinding in embryonic zebrafish exposed to nicotine. J Neurosci. 2002; 22:10731–10741. [PubMed: 12486166]
25. Pineda RH, Svoboda KR, Wright MA, Taylor AD, Novak AE, Gamse JT, Eisen JS, Ribera AB. Knockdown of Nav1.6a Na+ channels affects zebrafish motoneuron development. Development. 2006; 133:3827–3836. [PubMed: 16943272]
26. Ernst SG. A century of sea urchin development. Am Zool. 1997; 37:250–259.
27. Grant PT, Plack PA, Thomson RH. Gadusol, a metabolite from fish eggs. Tetrahedron Lett. 1980; 21:4043–4044.
28. Roy, S. Strategies for the minimization of UV-induced damage. In: de Mora, S.Demers, S., Vernet, M., editors. The Effects of UV Radiation in the Marine Environment, Cambridge Environmental Chemistry Series. Vol. 10. Cambridge University Press; New York: 2000. p. 206-236.
29. Kim DH, Hwang CN, Sun Y, Lee SH, Kim B, Nelson BJ. Mechanical analysis of chorion softening in prehatching stages of zebrafish embryos. IEEE Trans Nanobiosci. 2006; 5:89–94.
30. Morrison CM, Pohajdak B, Henry M, Wright JR. Structure and enzymatic removal of the chorion of embryos of the Nile tilapia. J Fish Biol. 2003; 63:1439–1453.
31. Zhang T, Rawson DM. Studies on chilling sensitivity of zebrafish (*Brachydanio rerio*) embryos. Cryobiology. 1995; 32:239–246.
32. Lahnsteiner F. The effect of internal and external cryoprotectants on zebrafish (*Danio rerio*) embryos. Theriogenology. 2008; 69:384–396. [PubMed: 18031801]

33. Browman HI, Vetter RD, Rodriguez CA, Cullen JJ, Davis RF, Lynn E, St Pierre JF. Ultraviolet (280–400 nm)-induced DNA damage in the eggs and larvae of *Calanus finmarchicus* G. (Copepoda) and Atlantic cod (*Gadus morhua*). Photochem Photobiol. 2003; 77:397–404. [PubMed: 12737142]
34. Legault R. A technique for controlling the time of daily spawning and collecting of eggs of the zebra fish, *Brachydanio rerio* (Hamilton-Buchanan). Copeia. 1958; 19:328–330.
35. Lamare MD, Barker MF, Lesser MP, Marshall C. DNA photorepair in echinoid embryos: effects of temperature on repair rate in Antarctic and non-Antarctic species. J Exp Biol. 2006; 209:5017–5028. [PubMed: 17142690]
36. Todo T, Ryo H, Takemori H, Toh H, Nomura T, Kondo S. High-level expression of the photorepair gene in Drosophila ovary and its evolutionary implications. Mutat Res. 1994; 315:213–228. [PubMed: 7526199]
37. Tamai TK, Vardhanabhuti V, Foulkes NS, Whitmore D. Early embryonic light detection improves survival. Curr Biol. 2004; 14:R104–R105. [PubMed: 14986634]
38. Kane DA, Kimmel CB. The zebrafish midblastula transition. Development. 1993; 119:447–456. [PubMed: 8287796]
39. Spemann H, Mangold H. Induction of embryonic primordia by implantation of organizers from a different species. 1923. Int J Dev Biol. 2001; 45:13–38. [PubMed: 11291841]

Appendix A. Supplementary data

Supplementary data associated with this article can be found, in the online version, at doi: 10.1016/j.jphotobiol.2008.07.011.

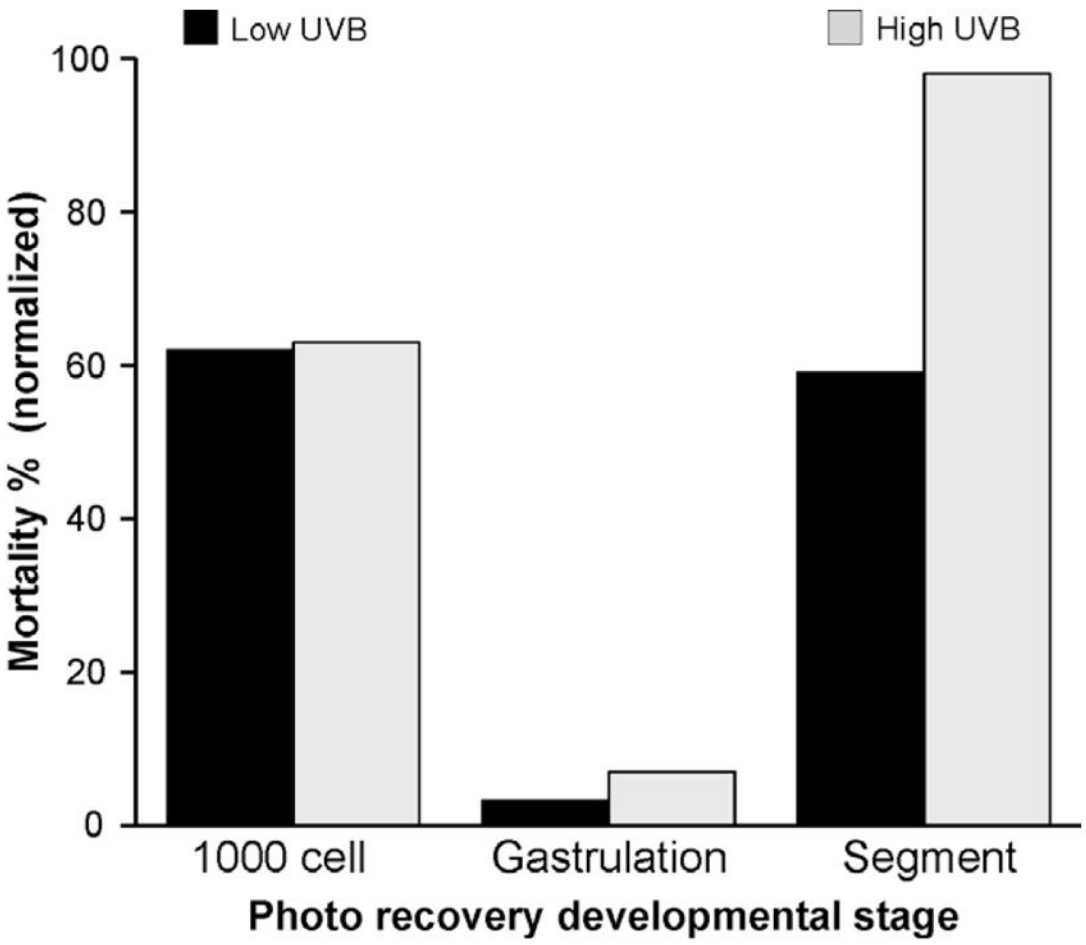

Fig. 1.

Photo recovery was most efficient at the gastrulation stage of development in pond-raised zebrafish embryos. Data are presented as normalized mortality percentages for embryos exposed to UV radiation at 3 hpf (1000 cell stage), 6–7 hpf (the mid-gastrula stage), and 12 hpf (segment stage) of development. Black bars, the mortality value caused by simultaneous exposure to UVB (1.56 J/cm^2) and UVA (211.5 J/cm^2 or 338.4 J/cm^2) was divided by the mortality value caused by exposure to UVB (1.56 J/cm^2) alone at each developmental stage. Photo recovery with 338.4 J/cm^2 UVA exposure following the 1.56 J/cm^2 UVB exposure at 3 hpf was not evaluated. Gray bars, the mortality value caused by the simultaneous exposure to UVB (3.11 J/cm^2) and UVA (338.4 J/cm^2) was divided by the mortality value caused by exposure to UVB (3.11 J/cm^2) alone at each developmental stage.

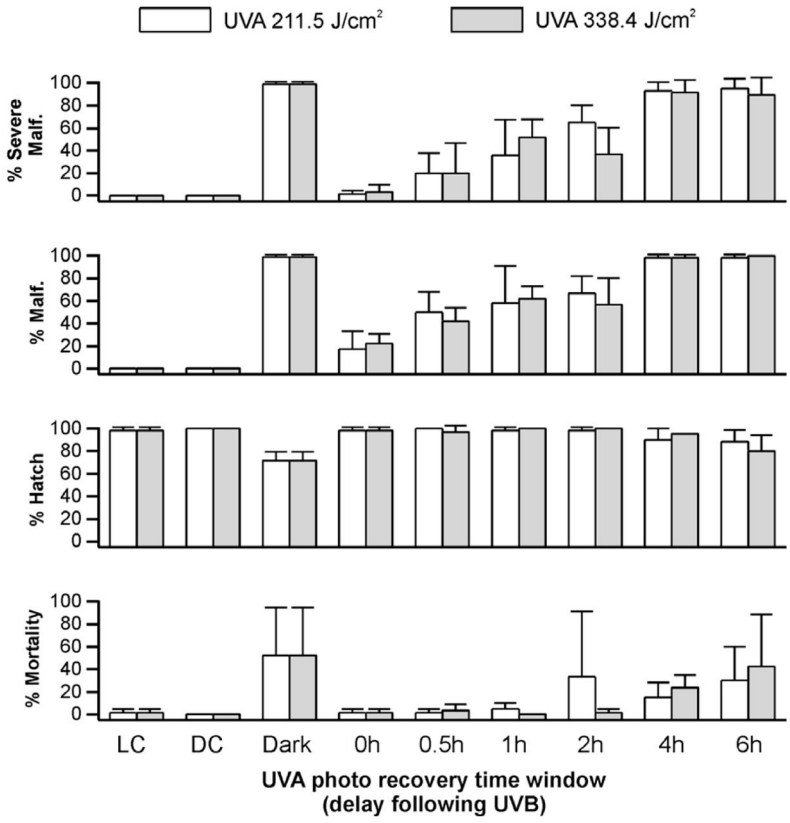

Fig. 2.

UVA-induced photo recovery time window in UVB-exposed (0.93 J/cm^2) zebrafish embryos. Percent hatch, mortality, malformation, and severe malformation of gastrulated zebrafish embryos within 5 days of exposure to UVB followed immediately (0 h) with UVA exposure at 211.5 J/cm^2 (white bars) and 338.4 J/cm^2 (gray bars) or incubated in dark for a period of 0.5 h, 1 h, 2 h, 4 h, and 6 h before UVA irradiation. Control embryos exposed to UVB without subsequent UVA irradiation were incubated in dark (Dark) for the first 20 h, and controls without UV irradiation were incubated in light (LC) or dark (DC) conditions.

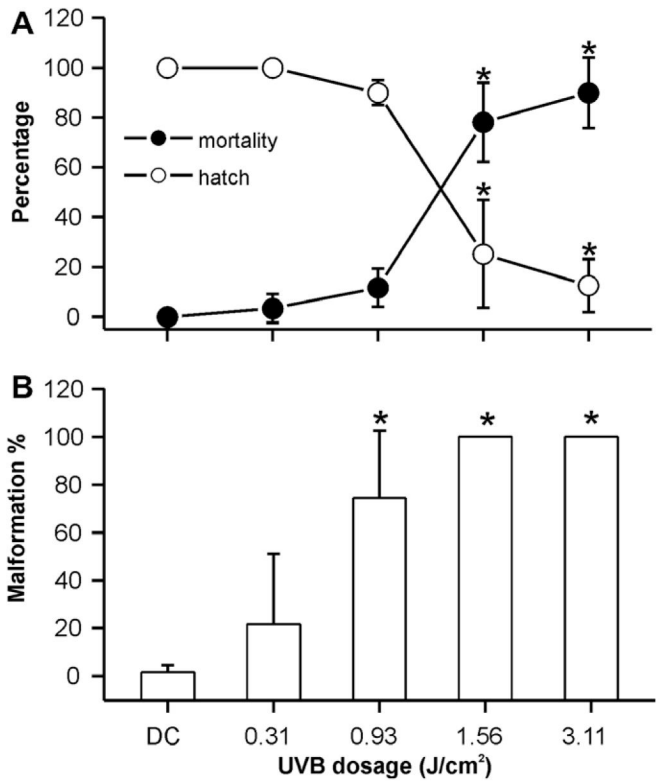

Fig. 3.

Dose–response for UVB exposure during mid-gastrulation in transgenic zebrafish (*fli-1*) embryos. (A) Percent hatch and mortality of embryos exposed to UVB during the mid-gastrulation stage of development within 5 days of the exposure. (B) Percent malformation of embryos exposed to UVB during the mid-gastrulation stage within 5 days of the exposure. Asterisks indicate a significant difference ($P < 0.05$) from control treatments without UV irradiation.

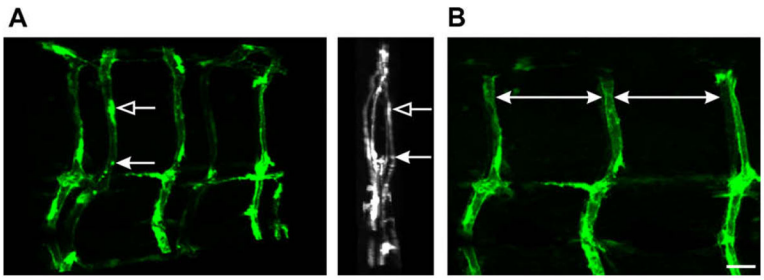

Fig. 4.

Vascular patterning in a larval *fli-1* zebrafish. (A) Left: z-stack projections where a *fli-1* larva has been optically sectioned (0.7 microns per section). The sections were projected and rotated. (A) Right: 90°-rotated projection presenting a midline view (anterior–posterior) of the projected image. The arrows indicate the same structure. (B) One side of the projection in A was rotated to provide a lateral view. The ISBVs in this projected view have a characteristic pattern of organization. The large white arrows denote the appearance of even spacing between ISBVs. Note in this lateral view the characteristic “S” shape of the ISBVs. Scale bar = 20 μm.

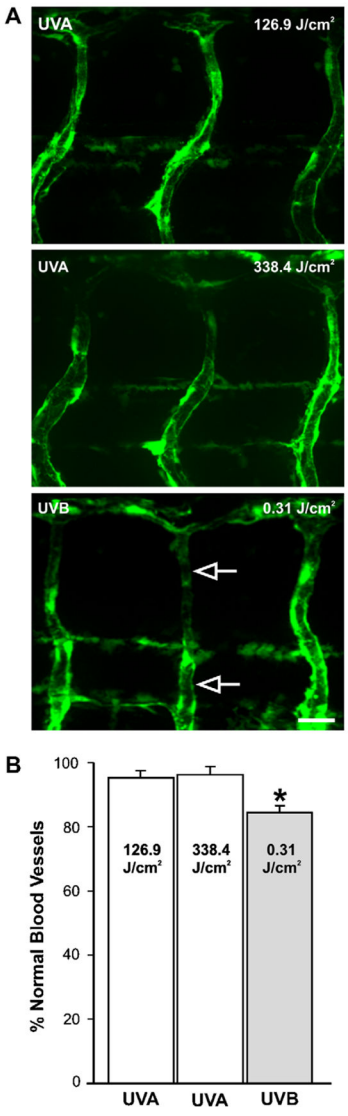

Fig. 5.

UV exposure in *fli-1* zebrafish embryos. (A) Photomicrographs of the vasculature from *fli-1* larvae that were exposed to UVA (top and middle) or UVB (bottom) during the mid-gastrulation stage of development. The open arrows point to an ISBV that projected in a straight trajectory along the dorsal–ventral axis. (B) Quantification in bar graph form indicating that a minimal UVB exposure altered ISBV development as 15 ± 2% of the vessels analyzed had abnormal morphologies (n = 15 larvae). UVA exposure of 126.9 and 338.4 J/cm^2 had no impact on ISBV morphology. Asterisk indicates significant difference (P < 0.05, ANOVA) in the number of normal vessels between the UVB-exposed and UVA exposed larvae. Scale bar = 20 μm.

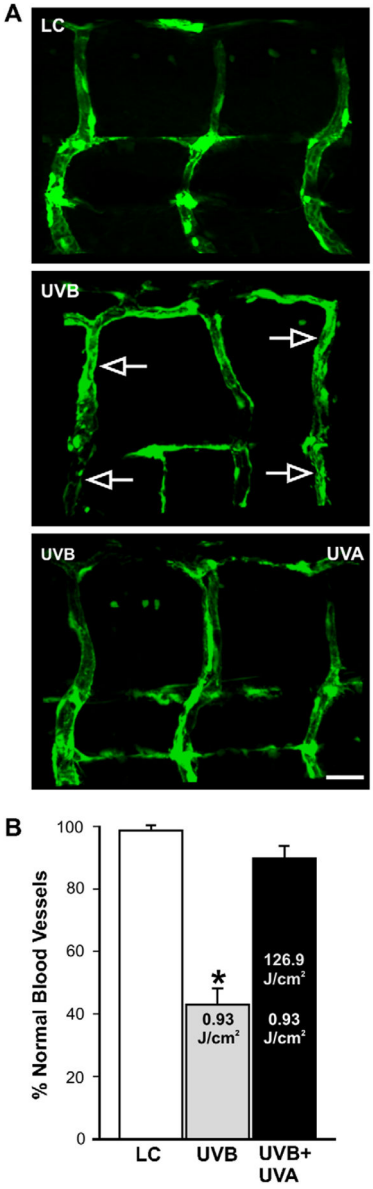

Fig. 6.

UVA-induced photo recovery in *fli-1* zebrafish embryos. (A) Photomicrographs of the vasculature from a *fli-1* larva that was not exposed to UV (Control, top), a *fli-1* larva exposed to 0.93 J/cm^2 UVB (middle), and a *fli-1* larva that was exposed to 0.93 J/cm^2 UVB followed by 126.9 J/cm^2 UVA (bottom) during the mid-gastrulation stage of development. Open arrows point to abnormal ISBVs which projected in a straight trajectory along the dorsal–ventral axis. (B) Quantification in bar graph form indicates that the UVA exposure elicited photo recovery as 91 ± 4% of the ISBVs had normal morphology (LC = light control). Asterisk indicates significant difference ($P < 0.05$, Student's *T*-Test) in the number of normal vessels between the UVB-exposed ($n = 23$) and the photo-recovered embryos ($n = 22$). Scale bar = 20 μm.

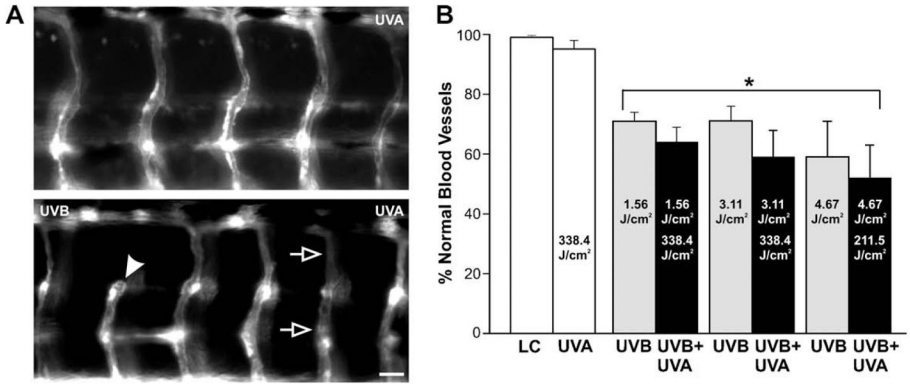

Fig. 7.

UVA-exposure did not induce photo recovery during the cleavage stage of development. (A) photomicrographs of the vasculature from a *fli-1* larva exposed to 338.4 J/cm^2 UVA (top) and a *fli-1* larva that was exposed to 1.56 J/cm^2-UVB followed by 338.4 J/cm^2 UVA (bottom) during the early cleavage stage of development (2–32 cell stage). The open arrows point to a straight ISBV. The arrowhead points to a region where a dorsal portion of the ISBV is absent. Images were obtained with a 20-× dry-objective to provide a wider field of view. B, Quantification in bar graph form indicates an inability of UVA exposure to recover abnormal ISBV morphology that occurred upon UVB exposure during the early cleavage stage of development. Asterisks indicate a significant difference from control embryos not exposed to UV irradiation ($P < 0.05$, ANOVA). A minimum of 9 larvae were analyzed for each experimental condition. Scale bar = 20 μm.

Table 1

UV exposure of embryos at 2–32 cell stage from wild-type (wild) and transgenic (*fli-1*) zebrafish

Fish source	UVB (J/cm^2)	UVA (J/cm^2)	Number of embryos	Mortality (%)	Hatch (%)	Malformation (%)	
						Total	Severe
Wild	4.67	0	40	5 ± 7	94 ± 8	19 ± 1	6 ± 0
	4.67	211.5	40	0 ± 0	100 ± 0	9 ± 12	6 ± 8
			R[a]	100	100	54	9
	6.22	0	100	23 ± 30	65 ± 42	55 ± 33	47 ± 34
	6.22	126.9	95	23 ± 29	58 ± 43	75 ± 34	60 ± 32
			R	3	20	0	0
fli-1	4.67	0	60	5 ± 9	93 ± 12	7 ± 6	2 ± 3
	4.67	211.5	60	30 ± 22	60 ± 33	5 ± 5	2 ± 4
			R	0	0	23	0
	6.22	0	170	20 ± 29	72 ± 29	35 ± 37	18 ± 19
	6.22	126.9	129	23 ± 29	69 ± 38	33 ± 35	32 ± 34
			R	0	0	6	0

Data were normalized with the non-exposed controls, and presented as mean ± SD.

[a]Percentage of recovery (*R*) was calculated based on the formula: $R = (t_1 - t_2)/t_1 \times 100$ for mortality and malformation, and $R = (t_2 - t_1)/(1 - t_1) \times 100$ for hatch where t_1 are means of UVB treatment only, and t_2 are means for treatment after UVA photo recovery; *R* was considered to be 0 when negative values occurred..